Interference of cold atoms released from an optical lattice

EUROPHYSICS LETTERS 1 November 2004

Europhys. Lett., **68** (3), pp. 330–336 (2004)
DOI: 10.1209/epl/i2004-10212-8

Interference of cold atoms released from an optical lattice

A. R. Kolovsky

Max-Planck-Institut für Physik Komplexer System - D-01187 Dresden, Germany and Kirensky Institute of Physics - 660036 Krasnoyarsk, Russia

received 5 May 2004; accepted in final form 7 September 2004
published online 6 October 2004

PACS. 03.75.-b – Matter waves.
PACS. 05.30.Jp – Boson systems.
PACS. 03.65.-w – Quantum mechanics.

Abstract. – We study interference of the cold atoms which are released out of the quasi–one-dimensional optical lattice, for the different initial states of the system. In particular, in the case of the Mott-insulator initial state, the atomic-density distribution is shown to exhibit a non-trivial interference pattern, similar to that observed for BEC in double-well potential in the experiment by Andrews *et al.* (*Science*, **275** (1997) 637).

Recently, much attention has been paid to Bose-Einstein condensate (BEC) of cold atoms, loaded in the optical lattices (see papers [1,2], and references therein). This interest is due to the fact that this system can realize different multiparticle states and (what is more important) these states can be relatively easily identified by using the so-called time-of-flight measurement technique. In the present paper, we theoretically study an interference pattern developed by atoms during their free flight. In the case of a coherent array of BECs (the superfluid state), typically realized in shallow lattices, this problem was addressed earlier in refs. [3,4]. Here we mainly focus on the opposite limit of deep lattices, where the initial state is Mott insulator. Because the Mott-insulator state (MI-state), unlike the superfluid state (SF-state), cannot be described by the macroscopic wave function, it is often treated as incoherent. In fact, the MI-state is a highly correlated state of the many-body system. We demonstrate below that these quantum correlations reveal themselves in a specific structure of the atomic-density distribution (as recorded by "taking a snapshot" of the expanding atomic cloud), which have not been discussed so far.

To understand how much the quantum correlations may affect the atomic-density distribution, let us analyze first a simpler problem of two colliding BEC [5,6]. Following ref. [5], we consider the state $|\Psi\rangle$ with equal number of atoms $N/2$ in each BEC, moving in the opposite directions with velocities $\pm p/M$; *i.e.*,

$$|\Psi\rangle = |(N/2)_+, (N/2)_-\rangle, \tag{1}$$

and the field operator

$$\hat{\Psi}(x) = \sum_{\pm} \frac{1}{\sqrt{L}} \exp\left[\pm i \frac{px}{\hbar}\right] \hat{a}_{\pm} \,. \tag{2}$$

The measured atomic-density distribution $N(x)$ is obviously given by

$$N(x) = \frac{1}{N}\sum_{n=1}^{N}\delta(x - x_n), \tag{3}$$

where the detected positions of the atoms x_n randomly vary in the repeated experiments, with the distribution function given by the square of the N-particle wave function of the system. One of the main results of paper [5] consists in constructing an effective numerical algorithm, which generates N random variables x_n according to the specified wave function (1). When N is increased, the atoms were found to have a tendency to clustering, and the coarse-grained atomic density,

$$\widetilde{N}(x) = \frac{1}{N}\int_{-\Delta x/2}^{\Delta x/2}\delta(x - x_n)\mathrm{d}x, \tag{4}$$

converges to

$$\widetilde{N}(x) = 1 - \cos(2px/\hbar + \phi), \tag{5}$$

with random phase ϕ.

Let us now show that the above correlations in the density $\widetilde{N}(x)$ can be predicted by analyzing the diagonal elements of the two-particle density matrix,

$$R(x_1, x_2) = \frac{1}{N(N-1)}\langle\Psi|\hat{\Psi}^\dagger(x_2)\hat{\Psi}^\dagger(x_1)\hat{\Psi}(x_1)\hat{\Psi}(x_2)|\Psi\rangle, \tag{6}$$

which give joint probability to find two atoms at the positions x_1 and x_2,

$$R(x_1, x_2) = \langle\langle N(x_1)N(x_2)\rangle\rangle \tag{7}$$

(here the double angular brackets denote an average over different realizations in the repeated experiments). Indeed, substituting (2) and (1) into eq. (6), we have

$$R(x_1, x_2) = \frac{N-2}{2(N-1)} + \frac{N}{N-1}\cos^2\left(\frac{p(x_2 - x_1)}{\hbar}\right). \tag{8}$$

It directly follows from eq. (8) that the recorded density distribution is modulated with the period $\pi\hbar/p$. If the number of the atoms in the BEC is large, this modulation can already be seen in the coarse-grained density $\widetilde{N}(x)$, as captured by eq. (5) and observed in the experiment [7]. In the opposite case of small N, one obviously needs many measurements to reveal the modulation. Let us also note that a structured two-particle density matrix together with a uniform one-particle density matrix $R(x) = 1$ implies the presence of random phase ϕ in eq. (5), which is often referred to as "the spontaneous breaking of the symmetry".

We proceed with the analysis of the two-particle density matrix for cold atoms in the optical lattice. Using the Wannier states $\psi_l(x)$ as single-particle basis wave functions, the field operator for spinless atoms in the optical lattice reads

$$\hat{\Psi}(x) = \sum_{l=1}^{L}\psi_l(x)\hat{a}_l\ , \quad \psi_l(x) = \psi_0(x - ld), \tag{9}$$

where L is the lattice size and d the lattice period. For the sake of completeness, we shall consider three different initial states of the system: the SF-state $|\Psi_{\mathrm{SF}}\rangle$, the MI-state for

repulsive atom-atom interactions $|\Psi_{\rm MI}^{(-)}\rangle$, and the superposition state $|\Psi_{\rm MI}^{(+)}\rangle$, which is the counterpart of the MI-state for attractive atom-atom interactions([1]):

$$|\Psi_{\rm SF}\rangle = \frac{1}{\sqrt{N!}}\left(\frac{1}{\sqrt{L}}\sum_{l=1}^{L} a_l^\dagger\right)^N |0\dots 0\rangle, \tag{10}$$

$$\left|\Psi_{\rm MI}^{(+)}\right\rangle = \frac{1}{\sqrt{L}}\sum_{l=1}^{L}\frac{1}{\sqrt{N!}}\left(a_l^\dagger\right)^N |0\dots 0\rangle, \tag{11}$$

$$\left|\Psi_{\rm MI}^{(-)}\right\rangle = \frac{1}{\sqrt{n!}}\prod_{l=1}^{L}\left(a_l^\dagger\right)^n |0\dots 0\rangle \tag{12}$$

(here $n = N/L$ is the filling factor). We also display the wave functions (10)-(12) in the coordinate representation for a particular case of $L = 2$ and $n = 1$ (generalization for arbitrary L and n is straightforward):

$$\begin{aligned}
\Psi_{\rm SF}(x_1, x_2) &= 2^{-1}[\psi_1(x_1) + \psi_2(x_1)][\psi_1(x_2) + \psi_2(x_2)],\\
\Psi_{\rm MI}^{(+)}(x_1, x_2) &= 2^{-1/2}[\psi_1(x_1)\psi_1(x_2) + \psi_2(x_1)\psi_2(x_2)],\\
\Psi_{\rm MI}^{(-)}(x_1, x_2) &= 2^{-1/2}[\psi_1(x_1)\psi_2(x_2) + \psi_1(x_2)\psi_2(x_1)].
\end{aligned}$$

The latter equations explicitly show that the SF-state is a product state, the "attractive MI-state" is a superposition of product states, while the repulsive MI-state is an entangled state.

Substituting (9) and (10)-(12) into eq. (6), we have the following expressions for the diagonal elements of the two-particle density matrix:

$$R_{\rm SF}(x_1, x_2) = \frac{1}{L^2}\left|\sum_l \psi_l(x_1)\right|^2 \left|\sum_l \psi_l(x_2)\right|^2, \tag{13}$$

$$R_{\rm MI}^{(+)}(x_1, x_2) = \frac{1}{L}\sum_l |\psi_l(x_1)|^2|\psi_l(x_2)|^2, \tag{14}$$

$$\begin{aligned}
R_{\rm MI}^{(-)}(x_1, x_2) = \frac{1}{L(L-1/n)}\Bigg[&\sum_{l\neq l'}|\psi_l(x_1)|^2|\psi_{l'}(x_2)|^2 + \left(1-\frac{1}{n}\right)\sum_l |\psi_l(x_1)|^2|\psi_l(x_2)|^2 +\\
&+\sum_{l\neq l'}\psi_l^*(x_1)\psi_{l'}(x_1)\psi_{l'}^*(x_2)\psi_l(x_2)\Bigg].
\end{aligned} \tag{15}$$

It is worth mentioning that by integration of the two-particle density matrix over one of the variables one obtains the one-particle density matrix, which is $R_{\rm SF}(x) = |\frac{1}{L}\sum_l \psi_l(x)|^2$ for the SF-state, and $R_{\rm MI}(x) = \frac{1}{L}\sum_l |\psi_l(x)|^2$ for both the superposition and MI-states.

Let us now demonstrate that the two-particle density matrix contains sufficient information to predict the outcome of a position measurement. The first row in fig. 1 shows the gray-scaled image of $R(x_1, x_2)$, given in eqs. (13)-(15), for $N = L = 7$ and the depth of the optical potential equal to 10 and 20 recoil energies for the SF- and MI-states, respectively.

([1])Note that the superposition state has never been realized in the laboratory experiments and, hence, the analysis of this situation serves mainly the pedagogical aims.

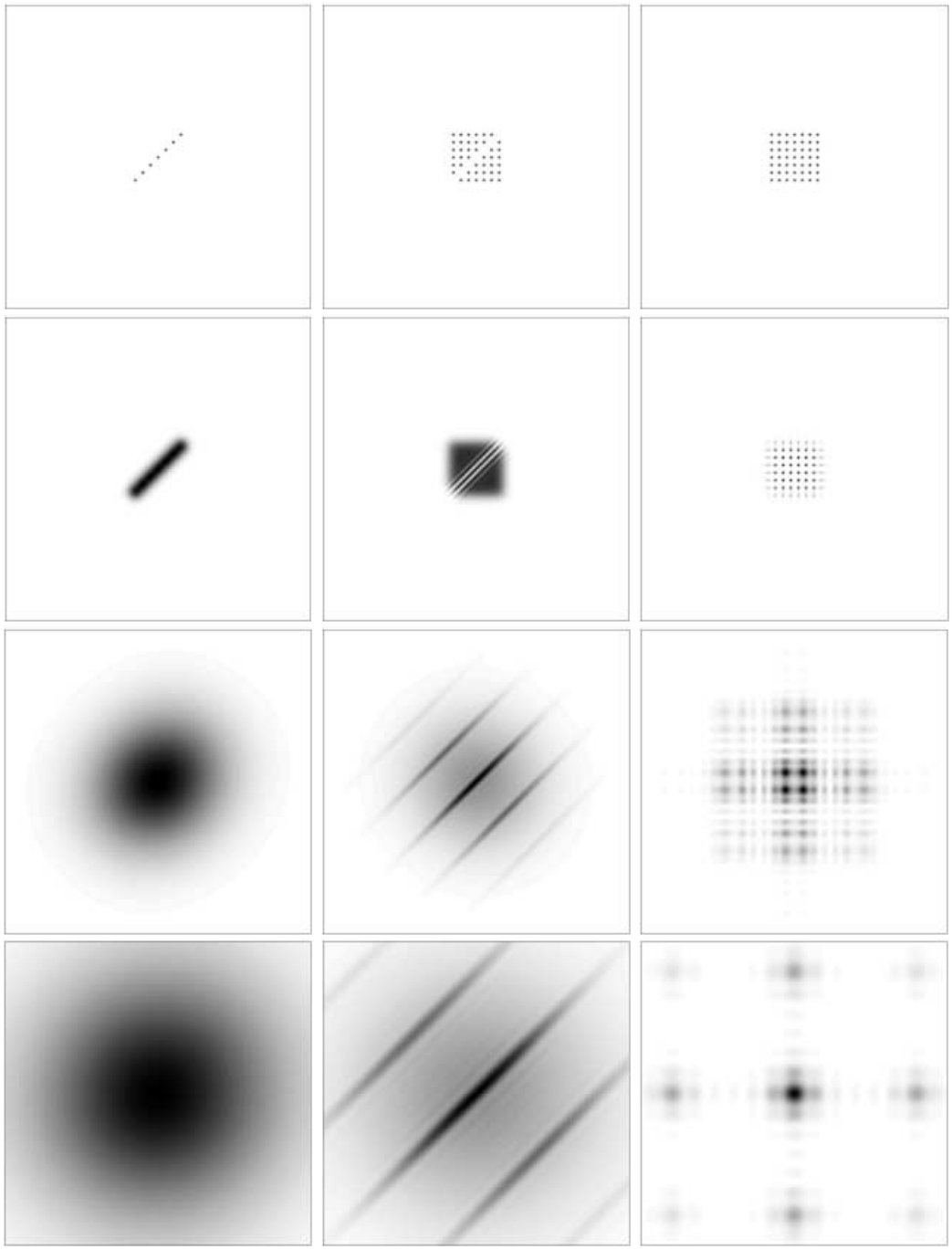

Fig. 1 – Gray-scaled image of the two-particle density matrix $R(x_1, x_2)$ for $N = 7$ atoms in the optical lattice with $L = 7$ wells (the axis limits are $-20d \leq x_1, x_2 \leq 20d$). The columns correspond to different initial conditions: the superposition state (11), left column; the Mott-insulator state (12), middle column; and the superfluid state (10), right column. The rows corresponds to different time-of-flight $t = 0, 1, 8, 16$ of the recoil periods.

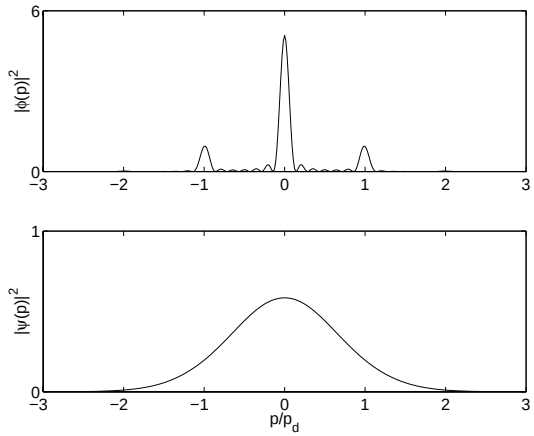

Fig. 2 – Momentum distributions of the Bloch state $\phi(x) = L^{-1/2} \sum_{l=1}^{L} \psi_l(x)$ (upper panel, $L = 7$) and Wannier states $\psi_l(x)$ (lower panel), $p_d = 2\pi\hbar/d$.

Three panels (from left to right) refer to the superposition state (11), the MI-state (12), and the SF-state (10). It is seen in the figure that in the case of the "attractive MI-state" (11) one has zero probability to find any two atoms in two different wells of the optical lattice. Thus, the position measurement will detect all atoms in a single well and $\widetilde{N}(x) = |\psi_l(x)|^2$, where the random index l breaks the spatial symmetry of the system, reflected in the uniform one-particle density matrix $R_{\mathrm{MI}}(x)$. Opposite to the case of attractive interaction, for the repulsive interaction (and $n = 1$), one has zero probability to find two atoms in one well. Thus the position measurement will result in $N(x) = \sum_l \delta(x - x_l)$, where x_l are chosen at random according to one-dimensional distributions $P_l(x) = |\psi_l(x)|^2$. Finally, in the case of the SF-state, one has an equal probability to find two atoms either in one well or in two different wells. Thus the atoms are distributed among the wells according to a binominal (Poisson, in the limit $N, L \to \infty$) law, while the distribution within a single well is defined by the square of the Wannier functions.

The above analysis of the outcome of a position measurement is obviously of pure academic interest, because the detection resolution in the laboratory experiments is essentially lower than the lattice period. To overcome this problem, the atoms are released out of the optical lattice and one waits for the atomic cloud to expand, before taking its image (which is a destructive measurement). We simulate the expansion of the atoms and the results are depicted in the subsequent rows of fig. 1 for $t = 1, 8, 16$ of the recoil periods. Note that in our simulations we neglected the collisions of the atoms during the expansion phase. Although we do not discuss here the formal condition for the validity of this approximation, the results of refs. [3, 7] indicate that this is indeed the case in the laboratory experiment.

Let us discuss fig. 1 in more detail. We begin with the SF-state (right column). First of all we note that, since the SF-state is a product state, the two-particle density matrix carries essentially the same information as single-particle wave function $\phi(x) = \frac{1}{\sqrt{L}} \sum_{l=1}^{L} \psi_l(x)$. Thus, a free expansion of the atomic cloud simply reveals the momentum distribution $|\phi(p)|^2$ of the Bloch state, which we depict in the upper panel of fig. 2.

The case of initial state $|\Psi_{\mathrm{MI}}^{(+)}\rangle$ (left column) is more complicated. Here the wave function is given by the coherent superposition of the product states and one may naively expect an interference. However, as seen in eq. (14), the structure of the two-particle density matrix

prohibits appearance of any interference pattern. Moreover, in the limit $t \to \infty$, the sum over l becomes irrelevant and $R^{(+)}_{\rm MI}(x_1, x_2; t) \approx |\psi_l(x_1, t)|^2 |\psi_l(x_2, t)|^2$. Thus an expansion of the atomic cloud reveals the momentum distribution $|\psi(p)|^2$ of the Wannier states,

$$\psi_l(x) = \frac{1}{2\pi\hbar} \int_{-\infty}^{\infty} \exp\left[-i\frac{px}{\hbar}\right] \psi(p) \exp\left[i\frac{l\,\mathrm{d}p}{\hbar}\right] \mathrm{d}p, \tag{16}$$

depicted in the lower panel of fig. 2.

The most complicated and interesting case is the MI-state (12). It is convenient to present the two-particle density matrix (15) as a sum of the "smooth" and "interference" parts:

$$R^{(-)}_{\rm MI}(x_1, x_2) = \frac{F(x_1, x_2) + |S(x_1, x_2)|^2}{L(L - 1/n)}, \tag{17}$$

$$S(x_1, x_2) = \sum_l \psi_l^*(x_1)\psi_l(x_2), \tag{18}$$

$$F(x_1, x_2) = \sum_{l \neq l'} |\psi_l(x_1)|^2 |\psi_{l'}(x_2)|^2 - \frac{1}{n} \sum_l |\psi_l(x_1)|^2 |\psi_l(x_2)|^2. \tag{19}$$

The time evolution of the smooth part (19) is asymptotically the same as for the superposition state (11), *i.e.*, in course of time it reveals the momentum distribution of the Wannier states. The time evolution of the interference part given by $|S(x_1, x_2)|^2$ is less trivial and can be qualitatively understood by considering the limit of an infinite lattice. Indeed, using the momentum representation (16) of the Wannier function, we obtain, in the limit $L \to \infty$,

$$S(x_1, x_2; t) = \sum_m \exp\left[-i\frac{m^2 M v^2}{2\hbar} t\right] S_m(x_2 - x_1 - mvt), \tag{20}$$

where

$$S_m(z) = \frac{1}{2\pi\hbar} \int \psi^*(p + mMv)\psi(p) \exp\left[-i\frac{zp}{\hbar}\right] \mathrm{d}p, \tag{21}$$

and $v = 2\pi\hbar/dM$ (M stands for atomic mass). Since the terms in eq. (19) have as their arguments the difference $z = x_2 - x_1 - mvt$, they produce a characteristic interference pattern seen in the middle column of fig. 1.

To summarize, we study the process of expansion of cold atoms, released out of an optical lattice. As already noticed earlier in refs. [1, 2] (and can be easily proved by analyzing the time evolution of the one-particle density matrix), the expansion reveals either the momentum distribution of the Bloch wave (the case of the superfluid initial state) or the momentum distribution of the Wannier function (the Mott-insulator initial state). Presented above more detailed, based on the two-particle density matrix, analysis shows that in the case of the Mott-insulator state one should additionally observe a specific interference pattern (*i.e.*, modulation of the recorded atomic density), captured by eqs. (17)-(21). We would like to note that this interference has essentially the same nature as that observed for BEC in double-well potential [7]. In fact, from the formal point of view the Mott-insulator state (12) is just an L-well generalization of the two-well state (1). We believe that the discussed interference can be observed in a laboratory experiment similar to [1], by adopting the "cross-section" detection technique of ref. [7], designed to eliminate the smearing effect of the transverse expansion of the atoms.

REFERENCES

[1] Orzel C., Tuchman A. K., Fenselau M. L., Yasuda M. and Kasevich M. A., *Science*, **291** (2001) 2386.
[2] Greiner M., Mandel O., Esslinger T., Hänsch T. W. and Bloch I., *Nature*, **415** (2002) 39.
[3] Pedri P., Pitaevskii L., Stringari S., Fort C., Burger S., Cataliotti F. S., Maddaloni P., Minardi F. and Inguscio M., *Phys. Rev. Lett.*, **87** (2001) 220401.
[4] Adhikari S. K. and Muruganandam P., *Phys. Lett. A*, **310** (2003) 229.
[5] Javanainen J. and Yoo S. M., *Phys. Rev. Lett.*, **76** (1996) 161.
[6] Naraschewski M., Wallis H., Schenzle A., Cirac J. I. and Zoller P., *Phys. Rev. A*, **54** (1996) 2185.
[7] Andrews M. R., Townsend C. G., Miesner H.-J., Durfee D. S., Kurn D. M. and Ketterle W., *Science*, **275** (1997) 637.